

Holographic non-Fermi liquid fixed points

BY TOM FAULKNER¹, NABIL IQBAL², HONG LIU², JOHN MCGREEVY² AND DAVID VEGH³

¹*KITP, Santa Barbara, CA 93106,*

²*Center for Theoretical Physics, Massachusetts Institute of Technology, Cambridge, MA 02139,*

³*Simons Center for Geometry and Physics, Stony Brook University, Stony Brook, NY 11794-3636*

Techniques arising from string theory can be used to study assemblies of strongly-interacting fermions. Via this ‘holographic duality’, various strongly-coupled many body systems are solved using an auxiliary theory of gravity. Simple holographic realizations of finite density exhibit single-particle spectral functions with sharp Fermi surfaces, of a form distinct from those of the Landau theory. The self-energy is given by a correlation function in an infrared fixed point theory which is represented by an AdS_2 region in the dual gravitational description. Here we describe in detail the gravity calculation of this IR correlation function.

This article is a contribution to a special issue of *Phil. Trans. A* on the normal state of the cuprates; as such, we also provide some review and context.

Keywords:

1. Introduction

The metallic states that we understand well are described by Landau Fermi liquid theory. This is a free stable RG fixed point (Benfatto & Gallavotti, 1990; Polchinski, 1992; Shankar, 1993) (modulo the BCS instability which sets in at parametrically low temperatures). Landau quasiparticles manifest themselves as (a surface of) poles in single-fermion Green’s function at $k_\perp \equiv |\vec{k}| - k_F = 0$

$$G_R(\omega, k) = \frac{Z}{\omega - v_F k_\perp + i\Gamma} + \dots \quad (1.1)$$

where the dots represent incoherent contributions. Landau quasiparticles are long-lived: their width is $\Gamma \sim \omega_\star^2$, where $\omega_\star(k)$ is the real part of the location of the pole. The residue Z , their overlap with the external electron, is finite on Fermi surface, and the spectral density becomes arbitrarily sharp there

$$A(\omega, k) \equiv \frac{1}{\pi} \text{Im} G_R(\omega, k) \xrightarrow{k_\perp \rightarrow 0} Z \delta(\omega - v_F k_\perp) \quad . \quad (1.2)$$

Thermodynamical and transport behavior of the system can be characterized in terms of these long-lived quasi-particles.

Non-Fermi liquid metals (NFL) exist but are mysterious; the ‘strange metal’ phase of optimally-doped cuprates is a notorious example. For example, data from angle-resolved photoemission (ARPES) in this phase (see (Damascelli *et al.*, 2003) and references therein) indicate gapless modes – the spectral function $A(\omega, k)$ exhibits nonanalyticity at $\omega \sim 0, k \sim k_F$ – around some k_F with width $\Gamma(\omega_\star) \sim \omega_\star$, and vanishing residue $Z \xrightarrow{k_\perp \rightarrow 0} 0$. Furthermore, the system’s resistivity exhibits a linear temperature dependence in sharp contrast to the quadratic dependence of a Fermi liquid. These anomalies, along with others, suggest that in the strange metal phase, there is still a sharp Fermi surface, but no long-lived quasiparticles.

Known field theoretical examples of non-Fermi liquids which also exhibit the phenomenon of a Fermi surface without long-lived quasi-particles include Luttinger liquids in 1+1 dimensions (Affleck, 1988), and a free fermion gas coupled to some gapless bosonic excitations, which can be either a transverse gauge field or certain order parameter fluctuations near a quantum critical point (see (Holstein *et al.*, 1973; Reizer, 1989; Baym *et al.*, 1990; Polchinski, 1993; Nayak & Wilczek, 1993; Halperin *et al.*, 1992; Altshuler *et al.*, 1994; Schafer & Schwenzer, 2004; Boyanovsky & de Vega, 2001; Lee & Nagaosa, 1992; Kim *et al.*, 1994; Oganesyan *et al.*, 2001; Lawler *et al.*, 2006; Nave & Lee, 2007; Lee, 2009; Metlitski & Sachdev, 2010; Mross *et al.*, 2010)). Neither of these, however, is able to explain the behavior of a strange metal phase. The former is specific to (1 + 1)-d kinematics. In the latter class of examples, the influence of gapless bosons is mostly along the forward direction, and is not enough, for example, to account for the linear temperature dependence of the resistivity.

Here we summarize recent findings of a class of non-Fermi liquids, some of which share similar low energy behavior to those of a strange metal phase, using the holographic approach (Liu *et al.*, 2009; Faulkner *et al.*, 2009a,b, 2010a,b) (see also (Lee, 2008; Cubrovic *et al.*, 2009; Rey, 2009)). One of the most intriguing aspects of these systems is that their low energy behavior is controlled by an infrared (IR) fixed point, which exhibits nonanalytical behavior only in the time direction. In particular, single-particle spectral function and charge transport can be characterized by the scaling dimension of the fermionic operator in the IR fixed point.

We should emphasize that at a microscopic level the systems we consider differ very much from the electronic systems underlying strange metals: they are translationally invariant and spherically symmetric; they typically involve a large number of fermions, scalars and gauge fields, characterized by a parameter N , and we have to work with the large N limit; at short distances, the systems approach a relativistic conformal field theory (CFT). Nevertheless, the similarity of their low energy behavior to that of a strange metal is striking and may not be an accident. After all, the key to our ability to characterize many-body systems has often been universalities of low energy physics among systems with different microscopies.

We should also mention that the holographic non-Fermi liquids we describe here likely reflect some intermediate-scale physics rather than genuine ground states. The systems in which they are embedded can have various superconducting (Gubser, 2008; Hartnoll *et al.*, 2008)[†] or magnetic (Iqbal *et al.*, 2010) instabilities, just as in real-life condensed matter systems.

In the next section we give a lightning introduction to holographic duality. The subsequent two sections describe the structure of the fermionic response in the simplest holographic realization of finite density. §5 is the core of this paper, where we describe in detail the calculation of the self-energy. In the final sections we comment on transport, the superconducting state, and a useful cartoon of the mechanism which kills the quasiparticles.

2. Holographic duality

The study of black holes has taught us that a quantum theory of gravity has a number of degrees of freedom that is sub-extensive. In general, one expects a gravitational system in some volume to be describable in terms of an ordinary quantum system living on the boundary. For a certain class of asymptotic geometries, these boundary degrees of freedom has been precisely identified (Maldacena, 1998; Witten, 1998; Gubser *et al.*, 1998). For a review of this ‘holographic duality’ in the present

[†] For a review see (Herzog, 2009) and (Horowitz, 2010).

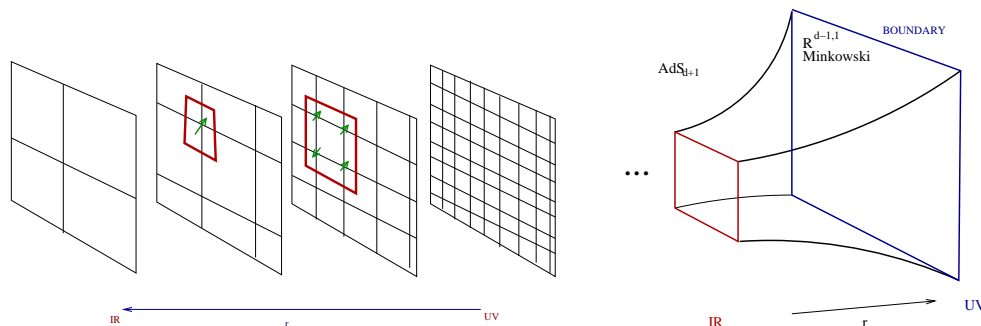


Figure 1. The left figure indicates a series of block spin transformations labelled by a parameter r . The right figure is a cartoon of AdS space, which organizes the field theory information in the same way. In this sense, the bulk picture is a hologram: excitations with different wavelengths get put in different places in the bulk image.

spirit, see (Sachdev & Mueller, 2008; Hartnoll, 2009a; McGreevy, 2009; Hartnoll, 2009b; Sachdev, 2010a).

The basic example of the duality is the following. A theory of gravity in $d + 1$ -dimensional Anti-de Sitter space, AdS_{d+1} , is a conformal field theory in d spacetime dimensions. Here by ‘is’ we mean that the observables are in one-to-one correspondence. AdS space,

$$ds^2 = \frac{r^2}{R^2} (-dt^2 + d\vec{x}^2) + R^2 \frac{dr^2}{r^2}, \quad (2.1)$$

can be viewed a collection of copies of Minkowski space $\mathbb{R}^{d,1}$ (whose isometries are the Poincaré group) of varying ‘size’, parametrized by a coordinate r . The isometries of AdS_{d+1} are precisely the conformal group in d spacetime dimensions. The ‘boundary’ where the dual field theory lives is at $r = \infty$ in these coordinates.

The extra (‘radial’) dimension can be considered as corresponding to the resolution scale for the dual theory. The evolution of the geometry (and the fields propagating therein) along this radial direction represent the RG flow of the dual field theory. The ‘AdS radius’, R in (2.1), is a dimensionful parameter which, roughly, encodes the rate of RG flow.

A practical consequence of this duality is the following equation for the field theory partition function:

$$\begin{aligned} Z_{QFT}[\text{sources}] &= Z_{\text{quantum gravity}}[\text{b. c. at } r \rightarrow \infty] \\ &\approx e^{-N^2 S_{\text{bulk}}[\text{b. c. at } r \rightarrow \infty]} \Big|_{\text{extremum of } S_{\text{bulk}}} \end{aligned} \quad (2.2)$$

The RHS of the first line is a partition function of quantum gravity, a general understanding of which is still lacking. The boundary conditions at $r \rightarrow \infty$ specify the sources in the QFT partition function. In the second line, the classical approximation to the quantum gravity partition function has been made via a saddle point approximation. The dimensionless parameter N^2 , which makes such an approximation possible, is the inverse of the Newton constant in units of curvature radius R , and is large in the classical limit. Through the duality, N^2 is mapped to the number of degrees of freedom per point in the dual free field theory. In the best-understood examples, the classical nature of the gravity theory arises from large- N factorization in the ‘t Hooft limit of a gauge theory.

Fields in AdS_{d+1} correspond to operators in CFT; the mass of the field determines the scaling dimension of the operator. The boundary conditions on a bulk field specifies the coefficient of the corresponding operator in the field theory action. For example, since the bulk theory is a gravitational theory, the bulk spacetime metric $ds^2 = g_{\mu\nu} dx^\mu dx^\nu$ is dynamical. The boundary value of bulk metric $\lim_{r \rightarrow \infty} g_{\mu\nu}$ is the source for the field theory stress-energy tensor $T^{\mu\nu}$. So we can rewrite (2.2) as

$$\langle e^{\phi_a^{(0)} \mathcal{O}^a} \rangle \approx e^{-N^2 S_{\text{bulk}}[\phi_a \xrightarrow{r \rightarrow \infty} \phi_a^{(0)}]} \Big|_{\text{extremum of } S_{\text{bulk}}} . \quad (2.3)$$

We can change the field theory action just by changing the *boundary conditions* on the bulk fields. Different couplings in the bulk action then correspond to entirely different field theories. For example, changing the bulk Newton constant (in units of curvature radius) is accomplished by changing the parameter N^2 ; but this is the number of degrees of freedom per point of the field theory.

In addition to large N^2 , useful calculation requires the background geometry to have small curvature. This is because otherwise we cannot reliably approximate the bulk action as

$$S = \int d^{d+1}x \sqrt{g} \left(\mathcal{R} + \frac{d(d+1)}{R^2} + \dots \right) \quad (2.4)$$

where \mathcal{R} is the Ricci scalar, and the ellipsis indicates terms with more powers of the curvature (and hence more derivatives). One necessary condition for this is that the ‘ AdS radius’ R be large compared to the energy scale set by the string tension. Given how it appears in (2.4), this requirement is a bulk version of the cosmological constant problem – the vacua with large cosmological constant require more information about the full string theory. The largeness of the dual geometry implies that the dual QFT is strongly coupled. Circumstantial evidence for this statement is that in QFTs which are weakly coupled we can calculate and tell that there is not a large extra dimension sticking out. The fact that certain strongly coupled field theories can be described by classical gravity on some auxiliary spacetime is extremely powerful, once we believe it.

(a) Confidence-building measures

Before proceeding to apply this machinery to non-Fermi liquid metals, we pause here to explain the reasons that give us enough confidence in these rather odd statements to try to use them to do physics. The reasons fall roughly into three categories

1. **Many** detailed checks have been performed in special examples. These checks have been done mainly in relativistic gauge theories (where the fields are $N \times N$ matrices) with extra symmetries (conformal invariance and supersymmetry). The checks involve so-called ‘BPS quantities’ (which are the same at weak coupling and strong coupling or which can be computed as a function of the coupling), integrable techniques, and more recently some numerics. We will not discuss any of these kinds of checks here, because they involve calculations of quantities which only exist in specific models, which neither the quantities nor the models are of interest here.
2. The holographic correspondence unfailingly gives sensible answers for physics questions. This includes rediscoveries of many known physical phenomena, some of which are quite hard to describe otherwise: *e.g.* color confinement, chiral symmetry breaking, thermo, hydro, thermal screening, entanglement entropy, chiral anomalies, superconductivity, ...

The gravity limit, when valid, says who are the correct variables, and gives immediate answers to questions about thermodynamics, transport, RG flow, ... in terms of geometric objects.

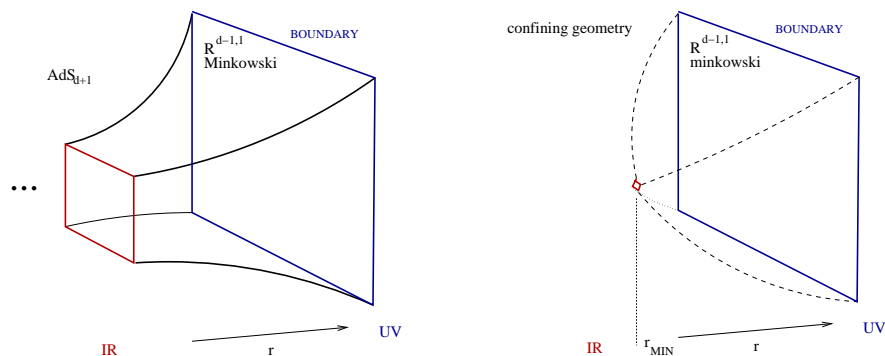


Figure 2. A comparison of the geometries associated with a CFT (left), and with a system with a mass gap (right).

3. If we are bold, the third class of reasons can be called “experimental checks”. These have arisen from applications to the quark-gluon plasma (QGP) produced at RHIC. Holographic calculations have provided a benchmark value for the viscosity of such a strongly-interacting plasma, and have provided insight into the behavior of hard probes of the medium, and of the approach to equilibrium.

As an illustration of the manner in which the correspondence solves hard problems by simple pictures we offer the following. The bulk geometry is a spectrograph separating the theory by energy scales. The geometry dual to a general Poincaré-invariant state of a QFT takes the form

$$ds^2 = w(r)^2 (-dt^2 + d\vec{x}^2) + R^2 \frac{dr^2}{r^2}. \quad (2.5)$$

For the gravity dual of a CFT, the bulk geometry goes on forever, and the ‘warp factor’ $w(r) = \frac{r}{R} \rightarrow 0$. On the other hand, in the gravity dual of a model with a gap, the geometry ends smoothly, warp factor $w(r)$ has a nonzero minimum value. If the IR region of the geometry is missing, there are no low-energy excitations and hence an energy gap in the dual field theory.

(b) Finite density

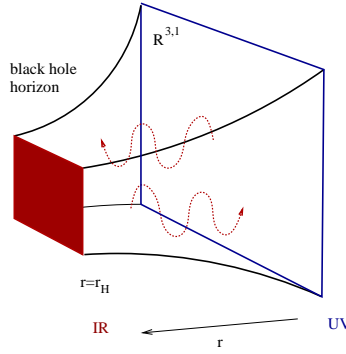
A basic question for the holographic description is how to describe a finite density. To approach this question, we introduce a minimal set of necessary ingredients in the bulk model. The fact that any local QFT has a stress tensor $T^{\mu\nu}$ means that we should have a dynamical metric $g_{\mu\nu}$ in bulk. As a proxy for the conserved fermion number, we assume that our QFT has a global abelian symmetry associated with a current j^μ ; this implies the presence of a massless gauge field A_μ in the bulk. As a proxy for bare electrons, we will also assume that our QFT includes a fermionic operator Ψ ; this leads us to introduce to a bulk spinor field ψ .

Consider any relativistic CFT with a gravity dual and a conserved $U(1)$ symmetry. The discussion goes through for any $d > 1 + 1$, but we focus on $d = 2 + 1$. The gravity dual is described by:

$$S = \frac{1}{2\kappa^2} \int d^d x \sqrt{g} \left(\mathcal{R} + \frac{6}{R^2} - \frac{2\kappa^2}{g_F^2} F_{\mu\nu} F^{\mu\nu} + \dots \right) \quad (2.6)$$

The ellipsis indicates fields which vanish in groundstate, and more irrelevant couplings. This is the action we would guess based on Wilsonian naturalness and it's what comes from string theory when we can compute it.

As a warmup, let's discuss the holographic description of finite temperature. The canonical ensemble of a QFT at temperature T is described by putting the QFT on a space with periodic Euclidean time of radius T^{-1} . The spacetime on which the dual QFT lives is the boundary of the bulk geometry at $r \rightarrow \infty$. So, the bulk description of finite temperature is the extremum of the bulk action whose Euclidean time has a period which approaches T^{-1} at the boundary. For many bulk actions, including (2.4), this saddle point is a black hole in AdS . This is a beautiful application of Hawking's observation that black holes have a temperature.



Similarly, the grand canonical ensemble is described by periodic Euclidean time with a Wilson line $e^{iq \oint_C A^{(0)}} = e^{-q\beta\mu}$ where C is the thermal circle, and $A^{(0)}$ is the background gauge field coupling to the current in question. The source $A^{(0)}$ is the boundary value of the bulk gauge field. For the minimal bulk field content introduced above, the bulk solution with these boundary conditions is the Reissner-Nördstrom (RN) black hole in AdS . We will comment below on how this conclusion is modified if we include other bulk fields, such as scalars, in (2.6).

For zero temperature, the solution of (2.6) describing a finite density of $U(1)$ charge is

$$ds^2 = \frac{r^2}{R^2} (-f dt^2 + d\vec{x}^2) + R^2 \frac{dr^2}{r^2 f}, \quad A = \mu \left(1 - \frac{1}{r} \right) dt \quad (2.7)$$

where $f(r) = 1 + \frac{3}{r^4} - \frac{4}{r^3}$ is the zero-temperature limit. This geometry has a horizon at $r = 1$. μ is the chemical potential for the $U(1)$ symmetry.

(c) *Strategy to find a Fermi surface*

To look for a Fermi surface, we look for sharp features in fermionic Green's functions at finite momentum and small frequency, following (Lee, 2008). Assume that amongst the ... in the bulk action (2.6) is†

$$S_{\text{probe}}[\psi] = \int d^{D+1}x \sqrt{g} (i\bar{\psi} (\not{D} - m) \psi + \text{interactions}) \quad (2.8)$$

† The derivative $\not{D} = \Gamma^M D_M$ contains the coupling to both the spin connection and the gauge field $D_M \equiv \partial_M + \frac{1}{4}\omega_{MAB}\Gamma^{AB} - iq_\psi A_M$.

The dimension and charge of the boundary fermion operator are determined by

$$\Delta = \frac{d}{2} + mR, \quad q = q. \quad (2.9)$$

Here we can see a kind of ‘bulk universality’: for two-point functions, the interaction terms don’t matter. We can describe many CFTs (many universality classes!) by a single bulk theory. The results only depend on q, Δ . Some comments on the strategy:

- There are many string theory vacua with these ingredients (Silverstein, 2004; Denef *et al.*, 2007; Douglas & Kachru, 2006; Grana, 2005; Denef, 2008). In specific examples of dual pairs (*e.g.* M2-branes \rightsquigarrow M-theory on $AdS_4 \times S^7$), the interactions and the parameters q, m are specified. Which sets $\{q, m\}$ are possible and what correlations there are is not clear, and, as an expedient, we treat them as parameters.
- This is a large complicated system (with a density $\rho \sim N^2$), of which we are probing a tiny part (the fermion density can be seen to scale like $\rho_\Psi \sim N^0$).
- In general, both bosons and fermions of the dual field theory are charged under the $U(1)$ current: this is a Bose-Fermi mixture. The relative density of bosons and fermions, and whether the bosons will condense, is a complicated dynamical question. Fortunately, the gravity theory solves this problem for us; let’s see what happens.

(d) *AdS/CFT prescription for spinors*

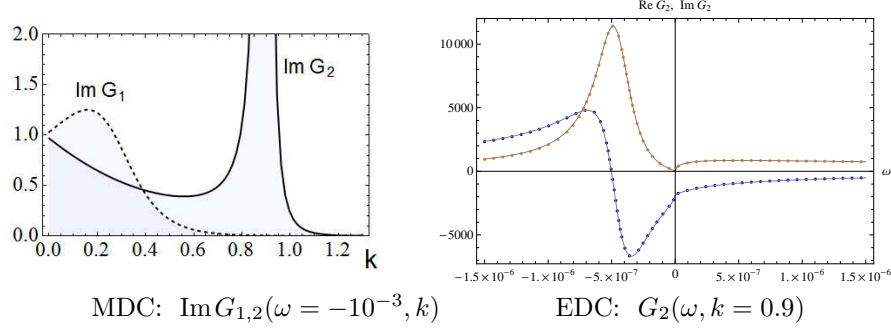
To compute the retarded single-fermion Green’s function G_R , we must solve the Dirac equation $(\not{D} + m)\psi = 0$ in the black hole geometry, and impose infalling boundary conditions at the horizon (Son & Starinets, 2002; Iqbal & Liu, 2009). Like retarded response, falling into the black hole is something that *happens*, rather than *unhappens*. Translation invariance in \vec{x}, t turns the Dirac equation into an ordinary differential equation in r . Rotation invariance allows us to set $k_i = \delta_i^1 k$; we can then choose a basis of gamma matrices in which the Dirac equation is block diagonal and real[†]. Near the boundary, solutions behave in this basis as

$$\Phi \stackrel{r \rightarrow \infty}{\approx} a_\alpha r^m \begin{pmatrix} 0 \\ 1 \end{pmatrix} + b_\alpha r^{-m} \begin{pmatrix} 1 \\ 0 \end{pmatrix} . \quad (2.10)$$

From this data, we can extract a matrix of Green’s functions, which has two independent eigenvalues:

$$G_\alpha(\omega, \vec{k}) = \frac{b_\alpha}{a_\alpha}, \quad \alpha = 1, 2 \quad (2.11)$$

The label $\alpha = 1, 2$ indexes a multiplicity which arises in the boundary theory as a consequence of the short-distance Lorentz invariance and will not be important for our purposes. The equation depends on q and μ only through $\mu_q \equiv \mu q$. We emphasize that all frequencies ω appearing below are measured from the effective chemical potential, μ_q . All dimensionful quantities below are quoted in units of the chemical potential.

MDC: $\text{Im}G_{1,2}(\omega = -10^{-3}, k)$ EDC: $G_2(\omega, k = 0.9)$

For $q = 1, m = 0$: $k_F \approx 0.918528499$

3. A Fermi surface

The system is rotation invariant, G depends on $k = |\vec{k}|$ and ω . The Green's function satisfies the following:

- The spectral density is positive for all ω as required by unitarity.
- The only non-analyticity in G_R (for real ω) occurs at $\omega = 0$. This could be anticipated on physical grounds, and is a consequence of the following argument. Consider a mode that is normalizable at the boundary, *i.e.* $a = 0$ in (2.10). This is a real boundary condition. Thus if the equations of motion are real (which they are for real ω), the wave must be real at the other end, *i.e.* at the horizon. Thus it must be a sum of both infalling and outgoing waves at the horizon. Thus it can't be an infalling solution. The exception is at $\omega = 0$ where the infalling and outgoing conditions are each real.
- The result approaches the CFT behavior at higher energies ($|\omega| \gg \mu$).

At $T = 0$, we find numerically a quasiparticle peak near $k = k_F \approx 0.9185$. The peak moves with dispersion relation $\omega \sim k_{\perp}^z$ with $z = 2.09$ for $q = 1, \Delta = 3/2$ and $z = 5.32$ for $q = 0.6, \Delta = 3/2$. There is scaling behavior near the Fermi surface

$$G_R(\lambda k_{\perp}, \lambda^z \omega) = \lambda^{-\alpha} G_R(k_{\perp}, \omega), \quad \alpha = 1. \quad (3.1)$$

It's not a Fermi liquid. The above scaling should be contrasted with the scaling in a Landau Fermi liquid, $z = \alpha = 1$. Finally, in the cases shown here, the residue vanishes at the Fermi surface.

4. Low-frequency behavior

So far, AdS/CFT is a black box which produces consistent spectral functions. To understand better where these numbers come from, we need to take apart the black box a bit.

† It is also convenient to redefine the independent variable by $\psi = (-\det gg^{rr})^{-1/4} \Phi$.

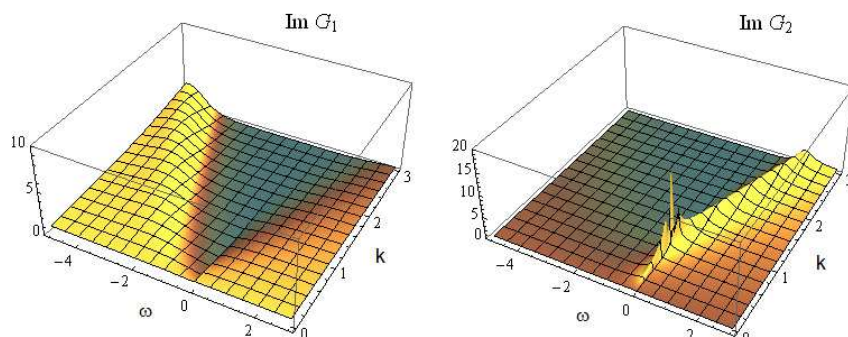


Figure 3. 3d plots of $\text{Im}G_1(\omega, k)$ and $\text{Im}G_2(\omega, k)$ for $m = 0$ and $q = 1$ ($\mu_q = \sqrt{3}$). In the right plot the ridge at $k \gg \mu_q$ corresponds to the smoothed-out peaks at finite density of the divergence at $\omega = k$ in the vacuum. As one decreases k to a value $k_F \approx 0.92 < \mu_q$, the ridge develops into an (infinitely) sharp peak indicative of a Fermi surface.

(a) *Emergent quantum criticality from geometry*

At $T = 0$, the ‘emblackening factor’ in (2.7) behaves as $f \approx 6(r - 1)^2$ and this means that the near-horizon geometry is $AdS_2 \times \mathbb{R}^{d-1}$. Recall that AdS means conformal symmetry. The conformal invariance of this metric is *emergent*. We broke the microscopic conformal invariance when we put in the finite density. AdS/CFT suggests that the low-energy physics is governed by the dual *IR CFT*. More precisely, there is such a CFT_0 for each \vec{k} . At small temperature $T \ll \mu$, the geometry is a black hole in AdS_2 times the space directions. The bulk geometry is a picture of the RG flow from the CFT_d to this non-relativistic CFT.

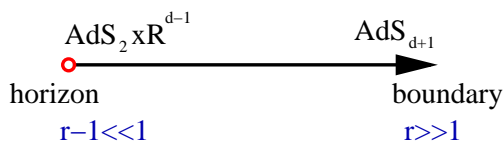


Figure 4. The geometry of the extremal AdS_{d+1} charged black hole.

(b) *Matching calculation*

At high temperatures (*i. e.* not small compared to the chemical potential) the retarded Green’s function $G_R(\omega)$ is analytic near $\omega = 0$, and can therefore be conveniently computed in series expansion (Son & Starinets, 2002). In the limit of interest to us, $T \ll \mu$, expanding the wave equation in ω is delicate. This is because the ω -term dominates near the horizon. We proceed using the method of matched asymptotic expansions: we find the solution (in an ω -expansion) in two regions of BH geometry (IR and UV), and fix integration constants by matching their behavior in the region of overlap. The region of overlap is large when $\omega, T \ll \mu$. This technique is familiar to string theorists from the brane absorption calculations (Aharony *et al.*, 2000) which led to the discovery of holographic duality. Here, this ‘matching’ can be interpreted in the QFT as RG

matching between UV and IR CFTs. Note that we need only assume the existence of the IR CFT; the gravity dual lets us compute.

First we discuss the IR boundary condition; this is associated with the near-horizon region of the bulk geometry, which is $AdS_2 \times \mathbb{R}^2$. Wave equations for charged fields in AdS_2 turn out to be solvable. Near the boundary of AdS_2 , the solutions for the mode with momentum k are power laws with exponents $\pm\nu_k$ where[†]

$$\nu_k \equiv R_2 \sqrt{m^2 + k^2 - q^2/2} \quad . \quad (4.1)$$

This exponent determines the scaling dimension of the IR CFT operator \mathcal{O}_k to which the spinor operator with momentum k flows: $\delta_k = \frac{1}{2} + \nu_k$. The retarded two-point function of the operator \mathcal{O}_k will play an important role, and is

$$\mathcal{G}_k(\omega) = c(k)\omega^{2\nu_k} \quad . \quad (4.2)$$

$c(k)$ is a complex function, whose calculation and explicit form is described in next section.

Next we consider the low-frequency expansion in the near-boundary region of the geometry, which is associated with the UV of the field theory. The outer region solutions can be expanded in powers of ω , and we can work in a basis where the Dirac equation is completely real. The UV data is therefore real and analytic in ω . A basis of solutions at $\omega = 0$ is

$$\Phi_\alpha^{(0)\pm} \stackrel{r \rightarrow 1}{\approx} v_\pm (r-1)^{\mp\nu} \quad (4.3)$$

where v_\pm are certain constant spinors which will be specified in Section 5 below. Two solutions can then be constructed perturbatively in ω :

$$\Phi_\alpha^\pm = \Phi_\alpha^{(0)\pm} + \omega\Phi_\alpha^{(1)\pm} + \omega^2\Phi_\alpha^{(2)\pm} + \dots, \quad \Phi_\alpha^{(n)\pm} \stackrel{r \rightarrow \infty}{\approx} \begin{pmatrix} b_\alpha^{(n)\pm} r^{-m} \\ a_\alpha^{(n)\pm} r^m \end{pmatrix}. \quad (4.4)$$

Matching these solutions to the leading and subleading solutions in the near-horizon region gives

$$\psi_\alpha = \psi_\alpha^+ + \mathcal{G}(\omega)\psi_\alpha^- \quad (4.5)$$

where \mathcal{G} is the IR CFT Green's function defined above in (4.2).

For any k , this produces a Green's function of the form:

$$\boxed{G_R(\omega, k) = K \frac{b_+^{(0)} + \omega b_+^{(1)} + O(\omega^2) + \mathcal{G}_k(\omega) \left(b_-^{(0)} + \omega b_-^{(1)} + O(\omega^2) \right)}{a_+^{(0)} + \omega a_+^{(1)} + O(\omega^2) + \mathcal{G}_k(\omega) \left(a_-^{(0)} + \omega a_-^{(1)} + O(\omega^2) \right)} \quad (4.6)}$$

The overall factor K will not be important in the following and we set it to unity. For generic k , the UV coefficient $a_+^{(0)}(k)$ is nonzero. The low-frequency expansion gives

$$G_R(\omega, k) = \frac{b_+^{(0)}}{a_+^{(0)}} + r_1\omega + r_2\mathcal{G}_k(\omega) + \dots \quad (4.7)$$

Since a_\pm, b_\pm are all real, we see that the nonanalytic behavior and dissipation are controlled by IR CFT.

[†] In the case of $d-1$ space dimensions, the formula becomes $\nu = R_2 \sqrt{m^2 + k^2 - q^2 e_d^2}$ where we define $e_d \equiv \frac{g_F}{\sqrt{2d(d-1)}}$.

(c) Consequences for Fermi surface

Suppose there is some $k = k_F$ such that $a_+^{(0)}(k_F) = 0$ in (4.6). This happens if there exists a zero-energy boundstate of outer-region Dirac equation; it could be called ‘inhomogeneous fermionic hair’ on the black hole. Near such a value of k ,

$$G_R(\omega, k) = \frac{h_1}{k_\perp - \frac{1}{v_F}\omega - h_2 c(k) \omega^{2\nu_{k_F}}}. \quad (4.8)$$

The coefficients $h_{1,2}, v_F$ are real, UV data. This form of the Green’s function correctly fits numerics near the Fermi surface. The expression (4.8) contains a lot of information about the behavior near the Fermi surface. The result depends on the value of ν compared to $\frac{1}{2}$.

First suppose $\frac{1}{2} > \nu_{k_F} \equiv \sqrt{m^2 + k_F^2 - q^2/2}/\sqrt{6}$. This means that the IR CFT operator \mathcal{O}_{k_F} is relevant, *i.e.* $\delta_{k_F} = \frac{1}{2} + \nu_{k_F} < 1$; we will explain the significance of this in the final section. This means that the non-analytic term dominates near $\omega = 0$:

$$G_R(\omega, k) = \frac{h_1}{k_\perp + \frac{1}{v_F}\omega + c_k \omega^{2\nu_{k_F}}} \quad \omega_*(k) \sim k_\perp^z, \quad z = \frac{1}{2\nu_{k_F}} > 1 \quad (4.9)$$

The excitation at the Fermi surface is not a stable quasiparticle:

$$\frac{\Gamma(k)}{\omega_*(k)} \xrightarrow{k_\perp \rightarrow 0} \text{const}, \quad Z \propto k_\perp^{\frac{1-2\nu_{k_F}}{2\nu_{k_F}}} \xrightarrow{k_\perp \rightarrow 0} 0. \quad (4.10)$$

Suppose $\nu_{k_F} > \frac{1}{2}$; in this case \mathcal{O}_{k_F} is irrelevant and the linear term dominates the dispersion:

$$G_R(\omega, k) = \frac{h_1}{k_\perp + \frac{1}{v_F}\omega + c_k \omega^{2\nu_{k_F}}} \quad \omega_*(k) \sim v_F k_\perp \quad (4.11)$$

There is a stable quasiparticle, but the system is not Landau Fermi liquid in that the lifetime goes like a funny power of frequency:

$$\frac{\Gamma(k)}{\omega_*(k)} \propto k_\perp^{2\nu_{k_F}-1} \xrightarrow{k_\perp \rightarrow 0} 0 \quad Z \xrightarrow{k_\perp \rightarrow 0} h_1 v_F. \quad (4.12)$$

Finally, suppose $\nu_{k_F} = \frac{1}{2}$: \mathcal{O}_{k_F} is *marginal*. The two frequency-dependent terms compete. $v_F \propto \nu_{k_F} - \frac{1}{2} \rightarrow 0$, while $c(k_F)$ has a pole; they cancel and leave behind a logarithm:

$$G_R \approx \frac{h_1}{k_\perp + \tilde{c}_1 \omega \ln \omega + c_1 \omega}, \quad \tilde{c}_1 \in \mathbb{R}, \quad c_1 \in \mathbb{C} \quad Z \sim \frac{1}{|\ln \omega_*|} \xrightarrow{k_\perp \rightarrow 0} 0. \quad (4.13)$$

This is the form of the Green’s function proposed in a well-named phenomenological model of the electronic excitations of the cuprates near optimal doping (Varma *et al.*, 1989).

The case $\nu_{k_F} = 1$ appears similar to a Landau Fermi liquid (Cubrovic *et al.*, 2009), though there are also logarithms in this case, and the physical origin of the quasiparticle decay is quite distinct from electron-electron interactions.

(d) *UV data: where are the Fermi surfaces?*

Above we assumed $a_+^{(0)}(k_F) = 0$. This happens at $k = k_F$ such that there exists a normalizable, incoming solution at $\omega = 0$. From a relativist's viewpoint, the black hole acquires inhomogeneous fermionic hair. By a change of variables, this problem can be translated into a boundstate problem in one-dimensional quantum mechanics. The relevant Schrödinger potentials are shown in Fig. 5. A few cases are worth noting. For $k > qe_d$, the potential is always positive and there can be

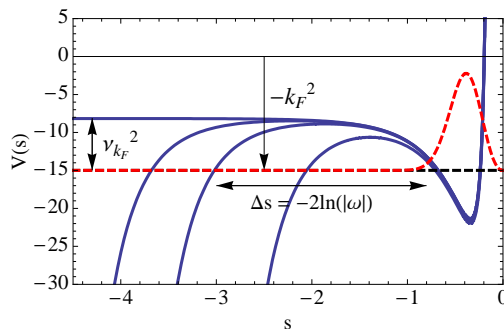


Figure 5. Shown here is a sequence of Schrödinger potentials for the scalar wave equation in the RN black hole. The horizontal axis is a ‘tortoise’ coordinate s which makes the wave equation into a one dimensional Schrödinger problem. The role of the energy in the Schrödinger problem is played by $-k^2$. The red dotted curve is a cartoon of the boundstate wavefunction at $\omega = 0$ with energy $-k_F^2$; the blue curve which becomes horizontal at large negative s (the IR region) is the associated Schrödinger potential for $\omega = 0$. As ω increases from zero, the potential develops a well in the IR region (the other blue curves), into which the boundstate can tunnel. The width of the barrier is $\Delta s \sim -2 \ln |\omega|$, and the height is $\nu_{k_F}^2$; hence the tunneling amplitude which determines the decay rate of the Fermi surface boundstate is $e^{-\text{area}} \sim \omega^{2\nu_{k_F}}$.

no boundstate; there is therefore no Fermi surface in this regime. Below a certain momentum, $k < k_{osc} \equiv \sqrt{(qe_d)^2 - m^2}$, the potential develops a singular well near the horizon $V(x) \sim \frac{\alpha}{r^2}$, with $\alpha < -\frac{1}{4}$. We refer to this as the ‘oscillatory regime’; it is associated with particle production in the AdS_2 region of the geometry. In this case, the exponent ν is imaginary, and hence G_R periodic in $\log \omega$. We note that this behavior is quite independent of the Fermi surface behavior.

In the intermediate regime $k \in (qe_d, k_{osc})$, the potential develops a well, indicating the possible existence of a zero energy bound state. The locations of these boundstates can easily be determined numerically and are shown in Fig. 6. Recently, such states have been shown to exist also for fields near black holes in asymptotically flat space (Hartman *et al.*, 2009).

(e) *Summary*

The location of the Fermi surface is determined by short-distance physics analogous to band structure – one must find a normalizable solution of $\omega = 0$ Dirac equation in full BH. The low-frequency scaling behavior near the Fermi surface however is universal; it is determined by near-horizon region and in particular the IR CFT \mathcal{G} . Depending on the dimension of the operator in the IR CFT, we find Fermi liquid behavior (but not Landau) or non-Fermi liquid behavior. From the bulk point of view, the quasiparticles decay by falling into the black hole. The rate at which they

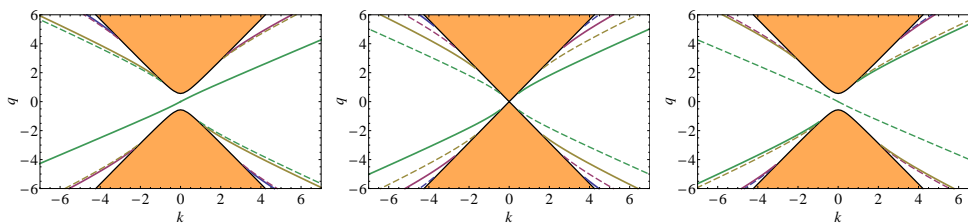


Figure 6. The values of q, k at which poles of the Green's function G_2 occur are shown by solid lines for $m = -0.4, 0, 4$. The dotted lines represent zeros of G_2 , and hence poles of the Green's function \tilde{G}_1 for the opposite sign of the mass. The orange bits indicate the oscillatory region, where $\nu \in i\mathbb{R}$.

fall in is determined by their effective mass (which by the correspondence determines the exponent ν) in the near-horizon region of the geometry.

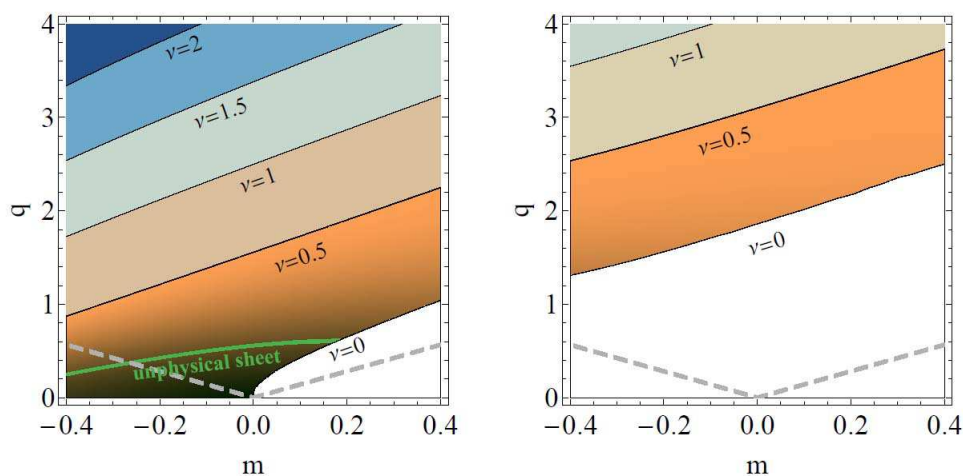


Figure 7. As we vary the mass and charge of the spinor field, we find the following behavior. In the white region, there is no Fermi surface. In the orange region, $\nu < \frac{1}{2}$ and we find non-Fermi liquid behavior. In the remainder of the parameter space, there is a stable quasiparticle.

5. Correlation functions in the AdS_2 IR CFT

Here we give a derivation of the retarded Green's function $\mathcal{G}(\omega)$ for a charged scalar and spinor in AdS_2 . We then describe the finite temperature case. Then we briefly discuss the generalization to other IR geometries.

The AdS_2 background metric and gauge field given by

$$ds^2 = \frac{R_2^2}{\zeta^2} (-d\tau^2 + d\zeta^2), \quad A = \frac{e_d}{\zeta} d\tau. \quad (5.1)$$

We describe below how the IR CFT correlators relevant to the calculations described above can be extracted from the behavior of fields in this background. One may worry that the nonzero profile of

the gauge field breaks the conformal invariance. In fact, conformal invariance is restored by acting simultaneously with a gauge transformation, as in (Hartman & Strominger, 2008).

(a) *Scalar*

We consider the following quadratic scalar action

$$S = - \int d^2x \sqrt{-g} [g^{ab}(\partial_a + iqA_a)\phi^*(\partial_b - iqA_b)\phi + m^2\phi^*\phi] \quad (5.2)$$

in the background (5.1). In frequency space $\phi(\tau, \zeta) = e^{-i\omega\tau}\phi(\omega, \zeta)$, the equation of motion for ϕ can be written as

$$-\partial_\zeta^2\phi + V(\zeta)\phi = 0 \quad (5.3)$$

with

$$V(\zeta) = \frac{m^2 R_2^2}{\zeta^2} - \left(\omega + \frac{qe_d}{\zeta}\right)^2. \quad (5.4)$$

Note ω can be scaled away by redefining ζ , reflecting the scaling symmetry of the background solution. Equation (5.3) can be solved exactly; the two linearly independent solutions are

$$\phi = c_{\text{out}} W_{iqe_d, \nu}(-2i\omega\zeta) + c_{\text{in}} W_{-iqe_d, \nu}(2i\omega\zeta), \quad (5.5)$$

where $W_{\lambda, \mu}(z)$ is the Whittaker function, and for scalars $\nu \equiv \sqrt{m^2 R_2^2 - q^2 e_d^2 + \frac{1}{4}}$. Of these, the function multiplying c_{in} , $W_{iqe_d, \nu}(-2i\omega\zeta) \sim e^{i\omega\zeta} \zeta^{iqe_d}$ is ingoing at the horizon.

Near the boundary of the AdS_2 region, the scalar solution behaves as

$$\phi \stackrel{\zeta \rightarrow 0}{\approx} A\zeta^{-\nu+\frac{1}{2}} + B\zeta^{\nu+\frac{1}{2}}. \quad (5.6)$$

The retarded scalar function of the IR CFT is then†

$$\mathcal{G}_R(\omega) = \frac{B}{A} = e^{-i\pi\nu} \frac{\Gamma(-2\nu)\Gamma(\frac{1}{2} + \nu - iqe_d)}{\Gamma(2\nu)\Gamma(\frac{1}{2} - \nu - iqe_d)} (2\omega)^{2\nu}. \quad (5.7)$$

The advanced function is given by

$$\mathcal{G}_A(\omega) = e^{i\pi\nu} \frac{\Gamma(-2\nu)\Gamma(\frac{1}{2} + \nu + iqe_d)}{\Gamma(2\nu)\Gamma(\frac{1}{2} - \nu + iqe_d)} (2\omega)^{2\nu}. \quad (5.8)$$

Now consider a charged scalar field on $AdS_2 \times \mathbb{R}^{d-1}$. In momentum space the equation of motion reduces to (5.4) with m^2 replaced by

$$m_k^2 \equiv k^2 \frac{R^2}{r_*^2} + m^2, \quad k^2 = |\vec{k}^2|. \quad (5.9)$$

Thus the retarded function is given by (5.7) with m^2 replaced by m_k^2 .

† Note that we define the scalar Green's function to be B/A without the prefactor of 2ν first emphasized in (Freedman *et al.*, 1999).

(b) Spinor

We consider the following quadratic action for a spinor field ψ in the geometry (5.1)

$$S_{\text{spinor}} = \int d^2x \sqrt{-g} i(\bar{\psi} \Gamma^a D_a \psi - m \bar{\psi} \psi + i \tilde{m} \bar{\psi} \Gamma \psi) ; \quad (5.10)$$

the last term in this action is a parity-violating mass term which in our application will be related to momentum in \mathbb{R}^{d-1} . We make the following choice of Gamma matrices, chosen to be compatible with the choice made in (Faulkner *et al.*, 2009a), with (5.1) arising as the near horizon limit

$$\Gamma^{\zeta} = \sigma^3, \quad \Gamma^{\tau} = i\sigma^1, \quad \Gamma = -\sigma^2 . \quad (5.11)$$

Then the equations of motion for ψ can be written as

$$(\zeta \partial_{\zeta} - i\sigma^3(\zeta\omega + qe_d)) \tilde{\Phi} = R_2 (m\sigma^2 + \tilde{m}\sigma^1) \tilde{\Phi} . \quad (5.12)$$

Here †

$$\tilde{\Phi} \equiv \begin{pmatrix} \tilde{y} \\ \tilde{z} \end{pmatrix} \equiv \frac{1}{\sqrt{2}} (1 + i\hat{\sigma}^1) (-gg^{\zeta\zeta})^{-1/4} \psi. \quad (5.13)$$

The general solution to this equation is

$$\tilde{\Phi}(\zeta) = \zeta^{-1/2} \left[c_{\text{out}} W_{-\frac{\sigma^3}{2} - iqe_d, \nu}(2i\omega\zeta) \begin{pmatrix} \tilde{m} - im \\ -1 \end{pmatrix} + c_{\text{in}} W_{\frac{\sigma^3}{2} + iqe_d, \nu}(-2i\omega\zeta) \begin{pmatrix} -1 \\ \tilde{m} + im \end{pmatrix} \right] \quad (5.14)$$

where again W is a Whittaker function, and where, for spinors, $\nu = \sqrt{m^2 R_2^2 - q^2 e_d^2}$. The notation σ^3 in the index of the Whittaker function indicates ± 1 when acting on the top/bottom component of the spinor.

The field which matches to the spinor field in the outer region is $\Phi = \frac{1}{\sqrt{2}}(1 - i\sigma^1)\tilde{\Phi}$. Near the boundary of AdS_2 , $\zeta \rightarrow 0$, the AdS_2 Dirac equation in this basis becomes

$$\zeta \partial_{\zeta} \Phi = U \Phi, \quad U = \begin{pmatrix} mR_2 & \tilde{m}R_2 - qe_d \\ \tilde{m}R_2 + qe_d & -mR_2 \end{pmatrix} . \quad (5.15)$$

The asymptotic behavior of Φ near the boundary of the AdS_2 region is as in equation (4.3):

$$\Phi = A v_- \zeta^{-\nu} (1 + O(\zeta)) + B v_+ \zeta^{\nu} (1 + O(\zeta)) \quad (5.16)$$

where v_{\pm} are real eigenvectors of U with eigenvalues $\pm\nu$. The relative normalization of v_+ and v_- is a convention, which affects the normalization of the AdS_2 Green's functions. We will choose v_{\pm} to be given by

$$v_{\pm} = \begin{pmatrix} mR_2 \pm \nu \\ \tilde{m}R_2 + qe_d \end{pmatrix} . \quad (5.17)$$

With the normalization convention in (5.17), the bottom components of v_{\pm} are equal and so A, B can be extracted from the asymptotics of z . The relative normalization of the eigenspinors in (5.17)

† There is a similar equation for the component which computes G_2 which is obtained by reversing the sign of the parity-violating mass \tilde{m} . From the point of view of the AdS_2 theory, this is a completely independent field.

affects the answer for the AdS_2 Green's function; $v_{\pm} \rightarrow \lambda_{\pm} v_{\pm}$ takes $\mathcal{G}_R \rightarrow \frac{\lambda_{\pm}}{\lambda_{\mp}} \mathcal{G}_R$. This rescaling does not, however, affect the full Green's function G_R computed by the matching procedure.

One then finds that the retarded Green's function of the operator coupling to y (the upper component of Φ) can be written as

$$\mathcal{G}_R(\omega) = e^{-i\pi\nu} \frac{\Gamma(-2\nu) \Gamma(1 + \nu - iqe_d)}{\Gamma(2\nu) \Gamma(1 - \nu - iqe_d)} \cdot \frac{(m - i\tilde{m}) R_2 - iqe_d - \nu}{(m - i\tilde{m}) R_2 - iqe_d + \nu} (2\omega)^{2\nu}. \quad (5.18)$$

The advanced function is given by

$$\mathcal{G}_A(\omega) = e^{i\pi\nu} \frac{\Gamma(-2\nu) \Gamma(1 + \nu + iqe_d)}{\Gamma(2\nu) \Gamma(1 - \nu + iqe_d)} \cdot \frac{(m + i\tilde{m}) R_2 + iqe_d - \nu}{(m + i\tilde{m}) R_2 + iqe_d + \nu} (2\omega)^{2\nu} \quad (5.19)$$

Now consider a charged fermion field on $AdS_2 \times \mathbb{R}^{d-1}$. Taking only $k_1 = k \neq 0$ dimensional reduction to (5.4) we find the action given by (5.10) with the identification $\tilde{m} = -k \frac{r_*}{R} (-1)^\alpha$.

(c) *Finite temperature generalization*

The above discussion can be generalized to finite temperature. In this case, the near horizon region is a (charged) black hole in AdS_2 (times space):

$$ds^2 = \frac{R_2^2}{\zeta^2} \left(- \left(1 - \frac{\zeta^2}{\zeta_0^2} \right) d\tau^2 + \frac{d\zeta^2}{1 - \frac{\zeta^2}{\zeta_0^2}} \right) + \frac{r_*^2}{R^2} d\vec{x}^2 \quad A = \frac{e_d}{\zeta} \left(1 - \frac{\zeta}{\zeta_0} \right) d\tau \quad (5.20)$$

and a temperature (with respect to τ) $T = \frac{1}{2\pi\zeta_0}$. Locally, this black hole in AdS_2 is related by a coordinate transformation (combined with a gauge transformation) to the vacuum AdS_2 , that is, it can be obtained by some global identifications. This fact can be used to infer the finite-temperature correlators from their zero-temperature limit presented above; they can also be determined directly as we do next.

The equation of motion for a minimally coupled scalar is

$$\partial_\zeta^2 \phi + \frac{2\zeta}{\zeta^2 - \zeta_0^2} \partial_\zeta \phi + \left(-\frac{m^2 R_2^2}{\zeta^2 - \frac{\zeta^4}{\zeta_0^2}} + \frac{\left[\omega + qe_d \left(\frac{1}{\zeta} - \frac{1}{\zeta_0} \right) \right]^2}{1 - \frac{2\zeta^2}{\zeta_0^2} + \frac{\zeta^4}{\zeta_0^4}} \right) \phi = 0.$$

Two linearly independent solutions are given by

$$\phi(\zeta) \sim \left(\frac{1}{\zeta} - \frac{1}{\zeta_0} \right)^{-\frac{1}{2} \mp \nu} \left(\frac{\zeta_0 + \zeta}{\zeta_0 - \zeta} \right)^{\frac{i\omega\zeta_0 - iqe_d}{2}} {}_2F_1 \left(\frac{1}{2} \pm \nu + i\omega\zeta_0 - iqe_d, \frac{1}{2} \pm \nu - iqe_d, 1 \pm 2\nu; \frac{2\zeta}{\zeta - \zeta_0} \right)$$

where $\nu = \sqrt{\frac{1}{4} + m^2 R_2^2 - q^2 e_d^2}$ and the top sign gives the ingoing solution.

Using $T = \frac{1}{2\pi\zeta_0}$, the scalar retarded Green's function has the following form

$$\mathcal{G}_R(\omega) = (4\pi T)^{2\nu} \frac{\Gamma(-2\nu) \Gamma\left(\frac{1}{2} + \nu - \frac{i\omega}{2\pi T} + iqe_d\right) \Gamma\left(\frac{1}{2} + \nu - iqe_d\right)}{\Gamma(2\nu) \Gamma\left(\frac{1}{2} - \nu - \frac{i\omega}{2\pi T} + iqe_d\right) \Gamma\left(\frac{1}{2} - \nu - iqe_d\right)}.$$

The spinor equation of motion at finite temperature is

$$\left(\partial_\zeta - i\hat{\sigma}^3 \frac{\omega + qA_\tau}{f}\right) \tilde{\Phi} = \frac{R_2}{\zeta\sqrt{f}} (m\hat{\sigma}^2 + \tilde{m}\hat{\sigma}^1) \tilde{\Phi} \quad (5.21)$$

where $\bar{f} \equiv 1 - \frac{\zeta^2}{\zeta_0^2}$ is the emblackening factor in the AdS_2 black hole metric in (5.20). It can similarly be solved in terms of hypergeometric functions. The general solution for the upper component \tilde{y} of $\tilde{\Phi}$ is

$$\begin{aligned} \tilde{y}(\zeta) = & \left(\frac{\zeta + \zeta_0}{\zeta}\right)^{\frac{1}{2} + i(qe_d + \frac{\zeta_0\omega}{2})} \\ & \left[c_{\text{in}} \left(-1 + \frac{\zeta_0}{\zeta}\right)^{-\frac{i\zeta_0\omega}{2}} {}_2F_1\left(\frac{1}{2} + iqe_d - \nu - i\zeta_0\omega, \frac{1}{2} + iqe_d + \nu - i\zeta_0\omega, \frac{1}{2} - i\zeta_0\omega, \frac{\zeta - \zeta_0}{2\zeta}\right) \right. \\ & \left. + c_{\text{out}} \left(-1 + \frac{\zeta_0}{\zeta}\right)^{\frac{i\zeta_0\omega}{2} + \frac{1}{2}} {}_2F_1\left(1 + iqe_d - \nu, 1 + iqe_d + \nu, \frac{3}{2} + i\zeta_0\omega, \frac{\zeta - \zeta_0}{2\zeta}\right) \right]. \end{aligned} \quad (5.22)$$

The retarded function is then

$$\mathcal{G}_R(\omega) = (4\pi T)^{2\nu} \frac{(m - i\tilde{m}) R_2 + iqe_d + \nu}{(m - i\tilde{m}) R_2 + iqe_d - \nu} \cdot \frac{\Gamma(-2\nu)\Gamma(\frac{1}{2} + \nu - \frac{i\omega}{2\pi T} + iqe_d)\Gamma(1 + \nu - iqe_d)}{\Gamma(2\nu)\Gamma(\frac{1}{2} - \nu - \frac{i\omega}{2\pi T} + iqe_d)\Gamma(1 - \nu - iqe_d)} \quad (5.23)$$

Note that the branch point at $\omega = 0$ of zero temperature now disappears and the branch cut is replaced at finite temperature by a line of poles parallel to the next imaginary axis. In the zero temperature limit the pole line becomes a branch cut. Similar phenomena have been observed previously (Festuccia & Liu, 2006).

(d) Finite temperature correlators and conformal invariance

In this subsection we describe how conformal invariance of the IR CFT actually completely fixes the frequency dependence of the finite temperature correlator derived above. The key point here, described in (Spradlin & Strominger, 1999), is that the AdS_2 black hole metric (5.20) is actually related to the $T = 0$ AdS_2 metric via a coordinate transformation that acts as a conformal transformation on the boundary of AdS_2 . To see this explicitly, consider the following coordinate transformation to a new set of coordinates (σ, t) :

$$\tau \pm \xi_0 \tanh^{-1}\left(\frac{\xi}{\xi_0}\right) = \xi_0 \log\left(\frac{t \pm \sigma}{\xi_0}\right). \quad (5.24)$$

Working out the metric (5.20) in these new coordinates we find eventually:

$$ds^2 = R_2^2 \frac{-dt^2 + d\sigma^2}{\sigma^2} \quad (5.25)$$

This is just the $T = 0$ AdS_2 metric, as claimed above. To better understand what happened consider the effect of the coordinate transformation (5.24) at the AdS_2 boundary $\sigma = \xi = 0$

$$t = \frac{1}{2\pi T} \exp(2\pi T\tau), \quad (5.26)$$

which is exactly the transformation that generates Rindler space in the τ coordinate from the vacuum in the t coordinate. This is simply the statement that a coordinate choice that defines a black hole in the AdS_2 bulk is equivalent to a coordinate choice that puts the field theory at a finite temperature. Because of conformal invariance this coordinate change is actually a symmetry operation in the IR CFT.

We note however that the gauge field adds a new subtlety; in particular, going through the same procedure with the zero temperature gauge field (5.1) does *not* give us the finite temperature gauge field (5.20). Let us go through the same steps as previously, starting this time with the zero temperature configuration appropriate to the metric (5.25):

$$A = \frac{e_d}{\sigma} dt \quad (5.27)$$

writing this in terms of the finite-temperature coordinates we obtain after some algebra

$$A = \frac{e_d}{\xi} d\tau + e_d d \left(\xi_0 \tanh^{-1} \left(\frac{\xi}{\xi_0} \right) \right) \quad (5.28)$$

Compare this to the gauge field configuration in (5.20). It is not the same, but the difference is pure gauge; indeed the gauge field \bar{A} defined by

$$\bar{A} = A + d\Lambda \quad \Lambda = -2\pi T e_d \tau - e_d \left(\xi_0 \tanh^{-1} \left(\frac{\xi}{\xi_0} \right) \right) \quad (5.29)$$

is exactly the gauge field appearing in the finite-temperature solution (5.20). Thus we have shown that the charged AdS_2 finite temperature black hole is precisely the same as a coordinate transform *plus* a gauge transform of the vacuum AdS_2 . Note that this gauge transform does not vanish at the AdS_2 boundary $\xi = 0$; the $d\tau$ part remains nonzero and corresponds to putting the IR CFT field theory at an (extra) constant value of A_τ .

Now the transformation of the IR CFT correlators under each of these manipulations is known; thus it should be possible to determine the finite temperature correlators from the $T = 0$ conformal results. For the conformal transformation (5.26) we use the usual CFT transformation law

$$\langle \mathcal{O}^\dagger(\tau) \mathcal{O}(\tau') \rangle = \left(\frac{dt}{d\tau} \right)^\delta \left(\frac{dt'}{d\tau'} \right)^\delta \langle \mathcal{O}^\dagger(t) \mathcal{O}(t') \rangle, \quad (5.30)$$

where $\delta = \frac{1}{2} + \nu$ is the dimension of the IR CFT operator.

The operation (5.29) is different and corresponds to turning on a source for the boundary gauge field that is pure gauge: generalizing slightly, in higher dimensions it would correspond to $A_\mu = \partial_\mu \Lambda$, with μ running over all field theory directions (in our case, only t). Thus with the insertion of this source we are now computing the field theory correlator

$$\langle \mathcal{O}^\dagger(x) \mathcal{O}(x') \rangle_\Lambda = \left\langle \exp \left(-i \int dy \Lambda(y) \partial_\mu j^\mu(y) \right) \mathcal{O}^\dagger(x) \mathcal{O}(x') \right\rangle \quad (5.31)$$

$\Lambda(x')$ has an effect on this correlator only because of the contact terms in correlation functions of the divergence of a current with a charged operator, e.g. $i \langle \partial_\mu j^\mu(y) \mathcal{O}(x) \rangle = iq \langle \mathcal{O}(x) \rangle \delta(x-y)$. In our case we find

$$\langle \mathcal{O}^\dagger(x) \mathcal{O}(x') \rangle_\Lambda = \exp(iq(\Lambda(x) - \Lambda(x'))) \langle \mathcal{O}^\dagger(x) \mathcal{O}(x') \rangle_{\Lambda=0} \quad (5.32)$$

Putting these ingredients together and using the fact that in the (t, σ) coordinate system we have just $\langle \mathcal{O}^\dagger(t)\mathcal{O}(t') \rangle \sim (t - t')^{-2\delta}$ we find

$$\langle \mathcal{O}^\dagger(\tau)\mathcal{O}(\tau') \rangle \sim \left(\frac{\pi T}{\sinh(\pi T(\tau - \tau'))} \right)^{2\delta} \exp(-2\pi i T e_d q(\tau - \tau')) \quad (5.33)$$

Here the first factor is simply the usual expression for a finite temperature correlator in the chiral half of a 2d CFT in a thermal ensemble, where the role of the coordinate of the ‘‘chiral half’’ is being played by the time coordinate. The extra factor is a new ingredient arising from the nontrivial sourcing of the gauge field. Upon Fourier transformation we should find the usual expression from 2d CFT at finite temperature (see e.g. (Iqbal & Liu, 2009; Birmingham *et al.*, 2002)), except with a shift in the frequency from the gauge field contribution:

$$\mathcal{G}(\omega) \sim (2\pi T)^{2\delta-1} \frac{\Gamma\left(\delta - \frac{i}{2\pi T}(\omega - 2\pi q e_d T)\right)}{\Gamma\left(1 - \delta - \frac{i}{2\pi T}(\omega - 2\pi q e_d T)\right)} \quad (5.34)$$

This frequency dependence agrees with that of the correlator derived directly from the bulk wave equation above.

6. Finite temperature

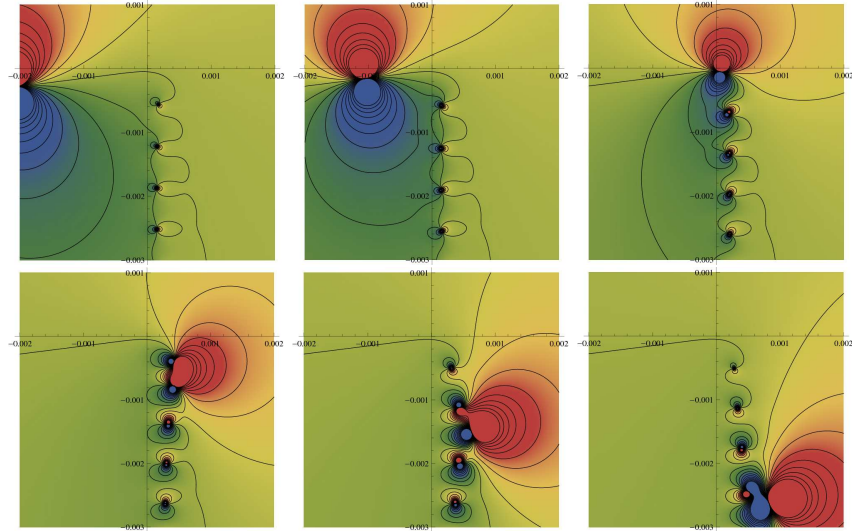
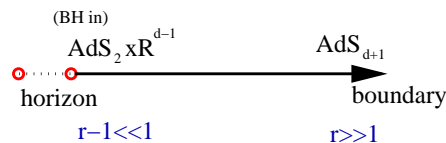


Figure 8. Density plots of $\text{Im}G_R$ in the complex frequency plane for a sequence of values of k near k_F , at finite temperature. The parameters are $m = 0$, $q = 1.23$, $T = 10^{-4}$ and this is the $\alpha = 2$ component; at $T = 0$ for these parameters, the Fermi surface lies at $k_F = 1.20554$. In the plots, $k_\perp = -0.01 \dots 0.03$.

At small nonzero temperature, the near-horizon geometry is a black hole in AdS_2 . Using the results for $\mathcal{G}(\omega, T)$ from Section 5c for the Green’s functions resulting from this IR geometry, the



fermion self energy becomes

$$\Sigma(\omega, T) = T^{2\nu} g(\omega/T) = (4\pi T)^{2\nu} \frac{\Gamma(\frac{1}{2} + \nu - \frac{i\omega}{2\pi T} + iqe_d)}{\Gamma(\frac{1}{2} - \nu - \frac{i\omega}{2\pi T} + iqe_d)} \xrightarrow{T \rightarrow 0} c_k \omega^{2\nu} \quad (6.1)$$

We first note from this formula (6.1) that what at $T = 0$ was a branch cut for $\omega^{2\nu}$ has become a line of discrete poles of the Gamma function.

An interesting phenomenon which occurs at $T = 0$ is that as $k \rightarrow k_F$, the quasiparticle pole sometimes moves under the branch cut and escapes onto another sheet of the complex ω plane; this leads to an extreme particle-hole asymmetry (visible in Fig 2C of (Faulkner *et al.*, 2010a)). More precisely, when the pole hits the branch point of $\mathcal{G}(\omega)$ at $\omega = 0$, it changes its ‘velocity’ $d\omega/dk$ according to $v_F(|\vec{k}| - k_F) = \mathcal{G}(\omega)$. Depending on the phase of \mathcal{G} , this can put the pole on another sheet of the complex omega plane.

This raises an interesting question: what happens to the pole which at $T = 0$ would have gone under the branch cut? The answer is that it joins the line of poles approximating the branch cut; their combined motion mimics the effects of the motion of the pole on the second sheet. This effect is visible in the sequence of pictures in Fig. 8.

At finite T , the pole no longer hits the real axis; the distance of closest approach is of order $(\pi T)^{2\nu}$. This is thermal smearing of the Fermi surface.

7. Discussion: charged AdS black holes and frustration

The state we have been studying has a large low-lying density of states. The entropy density of the black hole is

$$s(T = 0) = \frac{1}{V_{d-1}} \frac{A}{4G_N} = 2\pi e_d \rho . \quad (7.1)$$

At leading order in $1/N^2$, this is a large groundstate degeneracy. The state we are studying is not supersymmetric, and so we expect this degeneracy to be lifted at finite N . The most likely way in which the third law of thermodynamics will be enforced is by an instability to a superconducting state, the implementation and effects of which are discussed below in §9. In the absence of the necessary ingredients for a holographic superconductor, one way in which the degeneracy can be lifted was pointed out in (Hartnoll *et al.*, 2009). The groundstate of the spinor field in the Reissner-Nordström (RN) black hole is a Fermi sea of filled negative-energy states (a related discussion for a different black hole appears in (Hartman *et al.*, 2009)). An arbitrarily small density of matter close enough to the extremal horizon will produce an order-one back-reaction on the bulk geometry. According to (Hartnoll *et al.*, 2009), the density of spinor particles themselves modify the far-IR of the $AdS_2 \times \mathbb{R}^2$ to a Lifshitz geometry (Kachru *et al.*, 2008) with dynamical exponent $z \propto N^2$. This gravitating object, supported by the degeneracy pressure of charged fermions, has been called an ‘electron star’ (Hartnoll & Tavanfar, 2010). The modification occurs out to a very small distance from the horizon that scales like e^{-N^2} , and does not change the features of our calculations that we have emphasized above. (More concretely, the results are unchanged down to temperatures scaling

like e^{-N^2} .) If one considers instead spinor fields whose mass and charge grows with N (e.g. like $q \sim N$), then the back-reaction of a finite density can modify the geometry out to a larger radius of order $1/N$ to a Lifshitz background with a dynamical exponent which is finite in the large N limit (Hartnoll & Tavanfar, 2010).

We should comment in more detail on the effects on G_R of changes to the near-horizon geometry resulting from the gravitational back-reaction of the bulk fermion density (Hartnoll *et al.*, 2009; Faulkner & Polchinski, 2010). The geometry $AdS_2 \times \mathbb{R}^2$ discussed above is the $z \rightarrow \infty$ limit of the following family of metrics with Lifshitz scaling $t \rightarrow \lambda^z t, \vec{x} \rightarrow \lambda \vec{x}$:

$$ds^2 = \frac{R_2^2}{\zeta^2} (d\tau^2 + d\zeta^2) + \frac{r_*^2}{R^2} \zeta^{2/z} d\vec{x}^2 \quad (7.2)$$

Any finite z modifies the non-analytic behavior of the self-energy (Faulkner & Polchinski, 2010): The Lifshitz scaling implies that the IR CFT scaling function takes the form $\mathcal{G}_R(\omega, k) = \omega^{2\nu} F\left(\frac{\omega}{k^z}\right)$; note that it is k and not k_\perp that appears in the scaling function – the IR CFT knows nothing of k_F . Lifshitz wave equations for general z seem not to be exactly solvable, but at small frequency a WKB analysis can be used to study the scaling function more explicitly (Faulkner & Polchinski, 2010); the self-energy goes like $\exp\left(-1/\omega^{\frac{1}{z-1}}\right)$ for frequencies less than the scale at which the RN groundstate degeneracy is split. We emphasize that nevertheless the non-Fermi liquid behavior persists down to parametrically low energies (of order μe^{-z}).

There exist other geometries in which the ground entropy vanishes. For example, the inclusion of other light bulk modes (e.g. neutral scalars) (Herzog *et al.*, 2009; Gubser & Rocha, 2009; Goldstein *et al.*, 2009) can have an important effect on the groundstate. A systematic exploration of the fermion response in the general holographic description of finite density will be valuable.

(a) Fermions in the bulk and the oscillatory region

In this brief subsection we observe that some features of the ‘electron star’ are already visible in the fermion correlators computed in the RN black hole at leading order in $1/N$.

The electronic states in the curved background correspond to the solutions of the bulk Dirac equation with normalizable boundary conditions in the UV and regular boundary conditions (ingoing in Lorentzian signature) in the IR. The transverse momenta can be chosen continuously, $k_x, k_y \in \mathbb{R}$. In the radial r direction, there is no translational invariance, so in this direction we describe the wavefunction in real space. The radial quantum number n is discrete because boundary conditions have been specified. Finally, after fixing the transverse momenta, the frequency should be adjusted such that the solution satisfies the boundary conditions. This happens for ω values where the retarded Green’s function has a pole.

Instead of labeling the states by $\{k_x, k_y, n\}$ where n is the discrete radial quantum number, we can label them by $\{k_x, k_y, \omega\}$ where ω is chosen from the discrete set of poles of the retarded correlator with fixed k_x, k_y . The states will be automatically filled for $Re\omega < 0$ and empty for $Re\omega > 0$.

If there were translational invariance in the radial direction, then n would be a continuous parameter. When labeling the states by ω , this means that there is a continuum of poles in the correlator from which we can choose from. (In practice, the poles would probably form a branch cut.) In the bulk, deep inside the electron star there is locally a 3d Fermi surface. Since AdS/CFT should describe the excitations of the star, we expect infinitely many poles in the Green’s function for some values of the momenta.

Surprisingly, something like this already happens in the oscillatory region ($k < k_o$) in the Reissner-Nordström case. This is a regime of momenta where the Green’s functions are observed to have log-periodic behavior in frequency, and where the zero-frequency spectral weight is non-vanishing (Liu *et al.*, 2009). The basic observation is that although the poles do not yet form a branch cut, they do accumulate near $\omega = 0$. In tortoise coordinates one can see that exactly in this oscillatory region, the wavefunction “falls into the black hole”, *i.e.* it is localized in the IR.

We note further that in examples without an oscillatory region (as is the case for the alternative quantization, see the right part of Figure 5 of (Faulkner *et al.*, 2009a)), there is no bulk Fermi sea near the horizon, and therefore no such modification of the geometry. We must observe, however, that in known examples that have a Fermi surface but no oscillatory region, there is a relevant operator, perturbation by which removes the Fermi surface. It would be interesting to find a stable example without an oscillatory region.

8. Transport

The most prominent mystery of the strange metal phase is the linear-in- T electrical resistivity. Electron-electron scattering (combined with umklapp or impurities) produces $\rho \sim T^2$, electron-phonon scattering produces $\rho \sim T^5$. A van Hove singularity requires fine tuning of the Fermi level. No simple, robust effective field theory gives $\rho \sim T$.

AdS/CFT techniques are well-adapted for studying transport. Holographic conductivity is computed by solving Maxwell’s equations in the bulk. The answer is of the form

$$\sigma^{DC} = \lim_{\omega \rightarrow 0} \text{Im} \frac{1}{\omega} \langle j^x j^x \rangle(\omega, \vec{0}) = O(N^2) + N^0 \sigma_{\text{from spinor}} + \dots \quad (8.1)$$

The $O(N^2)$ contribution does not know about k_F as it only depends on the black hole geometry, and not on the dynamics of the fermions. The contribution to the conductivity from the holographic Fermi surface is down by N^{-2} : its extraction requires a (spinor) loop in the bulk, as in (Denef *et al.*, 2009a,b; Caron-Huot & Saremi, 2009).

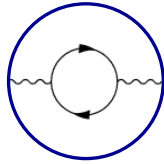


Figure 9. The ‘Witten diagram’ which gives the holographic Fermi surface contribution to the resistivity. The wiggly lines represent bulk gauge fields propagating from the boundary of AdS (dark blue circle); the solid lines represent bulk spinor propagators.

The result is very similar to the calculation of Fermi liquid conductivity (*e.g.* (Mahan, 2000)), with extra integrals over r , and no vertex corrections. The only process that contributes to leading order is depicted in Fig. 9. The key step is to relate the bulk spinor spectral function to that of the boundary fermion operator:

$$\text{Im} S_{\alpha\beta}(\Omega, k; r_1, r_2) = \frac{\psi_{\alpha}^b(\Omega, k, r_1) \bar{\psi}_{\beta}^b(\Omega, k, r_2)}{W_{ab}} A(\Omega, k) \quad (8.2)$$

where $A = \frac{1}{\pi} \text{Im} G_R$ is the spectral weight computed above. The conductivity is

$$\sigma^{DC} = S_d \int dk k^{d-2} \int d\omega \frac{df}{d\omega} \Lambda^2(k, \omega) A(\omega, k)^2 \quad (8.3)$$

f is the fermi function, and $\Lambda \sim q \int_{r_0}^{\infty} dr \sqrt{g} g^{xx} A_x(r, 0) \frac{\bar{\psi}^b(r) \Gamma^x \psi^b(r)}{W_{ab}}$ is a vertex factor, encoding data analogous to the UV coefficients $v_F, h_{1,2}$ in (4.8).

$$\sigma_{\text{from FS}}^{DC} = \Upsilon^2 k_F^{d-2} \int d\omega \frac{f'(\omega)}{\text{Im} \mathcal{G}(\omega)} \sim T^{-2\nu} \quad (8.4)$$

The factor Υ is determined by boundstate wavefunctions, k_F^{d-2} is the volume of the Fermi surface. In the last step we have used the scaling relation $\text{Im} \mathcal{G}(T \rightarrow 0, \omega/T \text{ fixed}) = T^{2\nu} g(\omega/T)$.

In the marginal Fermi liquid case where $\nu = \frac{1}{2}$, this indeed gives

$$\rho = (\sigma^{DC})^{-1} \sim T. \quad (8.5)$$

In contrast to the models of NFL that arise by coupling a Fermi surface to a gapless bosonic mode, the transport lifetime and the single-particle lifetime have the same temperature dependence. This is possible because the quasiparticle decay is mediated by the IR CFT, which contains low-energy modes for nonzero (indeed, for any) momentum.

Although the DC resistivity is not sensitive to the stability of the quasiparticles, the behavior of the optical conductivity does change dramatically at $\nu = \frac{1}{2}$ (Faulkner *et al.*, 2010a,b).

9. The superconducting state

A useful test of any model of the normal state is whether it can incorporate the transition to superconductivity. It is indeed possible to describe superconductivity holographically by including charged scalar fields in the black hole background. At low temperature, they can condense, spontaneously breaking the $U(1)$ symmetry, changing the background (Gubser, 2008; Hartnoll *et al.*, 2008).

The problem of the fermion response in various possible holographic superconducting phases has been studied in (Chen *et al.*, 2009; Faulkner *et al.*, 2009b; Gubser *et al.*, 2009, 2010; Ammon *et al.*, 2010; Benini *et al.*, 2010; Vegh, 2010). The superconducting condensate can open a gap in the fermion spectrum around the chemical potential (Faulkner *et al.*, 2009b) if a suitable bulk coupling between spinor and scalar is included. The bulk action we consider for the fermion is

$$S[\psi] = \int d^{d+1}x \sqrt{-g} [i\bar{\psi} (\Gamma^M D_M - m_\psi) \psi + \eta_5^* \varphi^* \psi^T C \Gamma^5 \psi + \eta_5 \varphi \bar{\psi} C \Gamma^5 \bar{\psi}^T] . \quad (9.1)$$

φ is the scalar field whose condensation spontaneously breaks the $U(1)$ symmetry. C is the charge conjugation matrix, and Γ^5 is the chirality matrix, $\{\Gamma^5, \Gamma^M\} = 0$. The superconducting order parameter in these studies is s-wave, but is not BCS.

Interestingly, in the condensed phase, one finds stable quasiparticles, even when $\nu \leq \frac{1}{2}$. The modes into which the quasiparticle decays in the normal state are lifted by the superconducting condensate. The quasiparticles are stable in a certain kinematical regime, similar to Landau's critical velocity for drag in a superfluid: these holographic superconductor groundstates do have gapless excitations (in fact a relativistic CFT worth), but the Fermi surface can occur outside their lightcone (visible as the blue dashed line in Fig. 10).

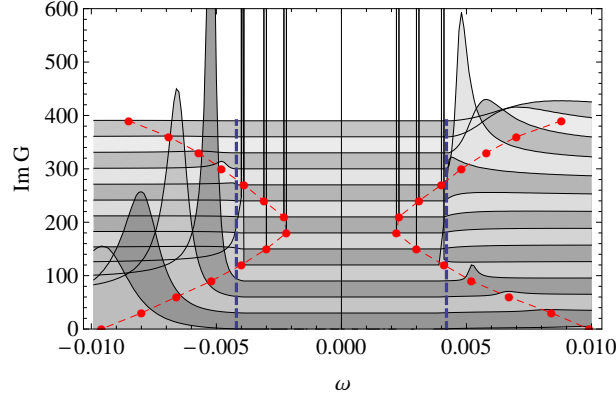


Figure 10. The effect of the superconducting order on the fermion spectral density (from (Faulkner *et al.*, 2009b)). Shown are plots of $A(k, \omega)$ at various $k \in [.81, .93]$ for $q_\psi = \frac{1}{2}, m_\psi = 0$ in a low-temperature background of a scalar with $q_\varphi = 1, m_\varphi^2 = -1$ (first constructed in (Horowitz & Roberts, 2009)), with $\eta_5 = 0.025$. The blue dashed line indicates the boundary of the region in which the incoherent part of the spectral density is completely suppressed, and the lifetime of the quasiparticle is infinite. The red dotted line indicates the location of the peak.

10. Conclusions

The holographic calculation of the spectral function can be described by a simple low energy effective theory (Faulkner *et al.*, 2009a; Faulkner & Polchinski, 2010; Faulkner *et al.*, 2010a,c). Consider a Fermi liquid (with creation operator ψ) mixing with a bath of critical fermionic fluctuations with large dynamical exponent:

$$L = \bar{\psi}(\omega - v_F k) \psi + \bar{\psi} \chi + \psi \bar{\chi} + \bar{\chi} \mathcal{G}^{-1} \chi \quad (10.1)$$

χ is an operator in the IR CFT; the k -independence of its correlations suggests that it arises from localized critical degrees of freedom. The corrected ψ Green's function is given by the geometric series:

$$\langle \bar{\psi} \psi \rangle = \frac{1}{\omega - v_F k - \mathcal{G}} \quad \mathcal{G} = \langle \bar{\chi} \chi \rangle = c(k) \omega^{2\nu}. \quad (10.2)$$

Note that according to the free fermion scaling, χ has dimension zero; therefore for $\nu \leq \frac{1}{2}$, the $\bar{\psi} \chi$ coupling is a relevant perturbation.

Above, we have described a certain class of fixed points which have some features in common with various non Fermi liquid metals. We find Fermi surfaces with vanishing quasiparticle residue. The single-fermion self-energy is a power-law in frequency, independent of momentum, as in DMFT and some slave-particle descriptions. Whether the states we describe can arise from any model of electrons with short-range interactions is an important open question[†].

[†] See (Sachdev, 2010b; Yamamoto & Si, 2010) for some recent ideas along this direction.

We thank T. Senthil for many useful discussions, and G. Horowitz and M. Roberts for collaboration on (Faulkner *et al.*, 2009b). Work supported in part by funds provided by the U.S. Department of Energy (D.O.E.) under cooperative research agreement DE-FG0205ER41360 and the OJI program, and in part by the National Science Foundation under Grant No. NSF PHY05-51164. The work of JM is supported in part by an Alfred P. Sloan Fellowship.

References

- I. Affeck, in *Fields, Strings and Critical Phenomena*, p. 563-640, (ed. E. Brzin and J. Zinn-Justin North-Holland, Amsterdam, 1990).
- O. Aharony, S. S. Gubser, J. M. Maldacena, H. Ooguri and Y. Oz, “Large N field theories, string theory and gravity,” *Phys. Rept.* **323**, 183 (2000) [arXiv:hep-th/9905111].
- B. L. Altshuler, L. B. Ioffe and A. J. Millis, “On the low energy properties of fermions with singular interactions,” arXiv:cond-mat/9406024.
- M. Ammon, J. Erdmenger, M. Kaminski and A. O’Bannon, “Fermionic Operator Mixing in Holographic p-wave Superfluids,” *JHEP* **1005**, 053 (2010) [arXiv:1003.1134 [hep-th]].
- G. Baym, H. Monien, C. J. Pethick, and D. G. Ravenhall, “Transverse interactions and transport in relativistic quark-gluon and electromagnetic plasmas,” *Phys. Rev. Lett.* **64** (1990) 1867.
- G. Benfatto and G. Gallavotti, “Renormalization-Group Approach to the Theory of the Fermi Surface,” *Phys. Rev. B* **42** (1990) 9967.
- F. Benini, C. P. Herzog and A. Yarom, “Holographic Fermi arcs and a d-wave gap,” arXiv:1006.0731 [hep-th].
- D. Birmingham, I. Sachs and S. N. Solodukhin, “Conformal field theory interpretation of black hole quasi-normal modes,” *Phys. Rev. Lett.* **88**, 151301 (2002) [arXiv:hep-th/0112055].
- D. Boyanovsky and H. J. de Vega, “Non-Fermi liquid aspects of cold and dense QED and QCD: Equilibrium and non-equilibrium,” *Phys. Rev. D* **63**, 034016 (2001) arXiv:hep-ph/0009172;
- S. Caron-Huot and O. Saremi, “Hydrodynamic Long-Time Tails from Anti De Sitter Space,” arXiv:0909.4525 [hep-th].
- J. W. Chen, Y. J. Kao and W. Y. Wen, “Peak-Dip-Hump from Holographic Superconductivity,” arXiv:0911.2821 [hep-th].
- M. Cubrovic, J. Zaanen and K. Schalm, “Fermions and the AdS/CFT correspondence: quantum phase transitions and the emergent Fermi-liquid,” arXiv:0904.1993 [hep-th].
- A. Damascelli, Z. Hussain, Z-X. Shen, “Angle-resolved photoemission studies of the cuprate superconductors,” *Rev. Mod. Phys.* **75**, 473 - 541 (2003).
- F. Denef, M. R. Douglas and S. Kachru, “Physics of string flux compactifications,” *Ann. Rev. Nucl. Part. Sci.* **57**, 119 (2007) [arXiv:hep-th/0701050];
- F. Denef, “Les Houches Lectures on Constructing String Vacua,” arXiv:0803.1194 [hep-th].
- F. Denef, S. A. Hartnoll and S. Sachdev, “Quantum Oscillations and Black Hole Ringing,” arXiv:0908.1788 [hep-th].
- F. Denef, S. A. Hartnoll and S. Sachdev, “Black Hole Determinants and Quasinormal Modes,” arXiv:0908.2657 [hep-th].
- M. R. Douglas and S. Kachru, “Flux compactification,” *Rev. Mod. Phys.* **79**, 733 (2007) [arXiv:hep-th/0610102];
- T. Faulkner, H. Liu, J. McGreevy and D. Vegh, “Emergent Quantum Criticality, Fermi Surfaces, and AdS_2 ,” arXiv:0907.2694 [hep-th];

- T. Faulkner, G. T. Horowitz, J. McGreevy, M. M. Roberts and D. Vegh, “Photoemission ‘Experiments’ on Holographic Superconductors,” arXiv:0911.3402 [hep-th].
- T. Faulkner and J. Polchinski, “Semi-Holographic Fermi Liquids,” arXiv:1001.5049 [hep-th].
- T. Faulkner, N. Iqbal, H. Liu, J. McGreevy and D. Vegh, “Strange Metal Transport Realized by Gauge/Gravity Duality” **Science**, Vol. 329. no. 5995 (2010) 1043 [arXiv:1003.1728 [hep-th]].
- T. Faulkner, N. Iqbal, H. Liu, J. McGreevy and D. Vegh, “Charge transport by holographic non-Fermi liquids” to appear.
- T. Faulkner, H. Liu and M. Rangamani, “Integrating out geometry: Holographic Wilsonian RG and the membrane paradigm,” arXiv:1010.4036 [hep-th].
- G. Festuccia and H. Liu, “Excursions beyond the horizon: Black hole singularities in Yang-Mills theories. I,” **JHEP** **0604**, 044 (2006) [arXiv:hep-th/0506202].
- D. Z. Freedman, S. D. Mathur, A. Matusis and L. Rastelli, “Correlation functions in the $CFT(d)/AdS(d+1)$ correspondence,” **Nucl. Phys. B** **546**, 96 (1999) [arXiv:hep-th/9804058].
- K. Goldstein, S. Kachru, S. Prakash and S. P. Trivedi, “Holography of Charged Dilaton Black Holes,” arXiv:0911.3586 [hep-th].
- M. Grana, “Flux compactifications in string theory: A comprehensive review,” **Phys. Rept.** **423**, 91 (2006) [arXiv:hep-th/0509003];
- S. S. Gubser, I. R. Klebanov and A. M. Polyakov, “Gauge theory correlators from non-critical string theory,” **Phys. Lett. B** **428**, 105 (1998).
- S. S. Gubser, “Breaking an Abelian gauge symmetry near a black hole horizon,” **Phys. Rev. D** **78**, 065034 (2008) [arXiv:0801.2977 [hep-th]];
- S. S. Gubser and F. D. Rocha, “Peculiar Properties of a Charged Dilatonic Black Hole in AdS_5 ,” arXiv:0911.2898 [hep-th].
- S. S. Gubser, F. D. Rocha and P. Talavera, “Normalizable Fermion Modes in a Holographic Superconductor,” arXiv:0911.3632 [hep-th].
- S. S. Gubser, F. D. Rocha and A. Yarom, “Fermion correlators in non-abelian holographic superconductors,” arXiv:1002.4416 [hep-th].
- B. I. Halperin, P. A. Lee and N. Read, “Theory of the half filled Landau level,” **Phys. Rev. B** **47**, 7312 (1993).
- T. Hartman and A. Strominger, “Central Charge for AdS_2 Quantum Gravity,” **JHEP** **0904**, 026 (2009) [arXiv:0803.3621 [hep-th]].
- T. Hartman, W. Song and A. Strominger, “The Kerr-Fermi Sea,” arXiv:0912.4265 [hep-th].
- S. A. Hartnoll, C. P. Herzog and G. T. Horowitz, **Phys. Rev. Lett.** **101**, 031601 (2008) [arXiv:0803.3295 [hep-th]], **JHEP** **0812**, 015 (2008) [arXiv:0810.1563 [hep-th]];
- S. A. Hartnoll, “Lectures on Holographic Methods for Condensed Matter Physics,” arXiv:0903.3246 [hep-th].
- S. A. Hartnoll, “Quantum Critical Dynamics from Black Holes,” arXiv:0909.3553 [cond-mat.str-el].
- S. A. Hartnoll, J. Polchinski, E. Silverstein and D. Tong, “Towards Strange Metallic Holography,” arXiv:0912.1061 [hep-th].
- S. A. Hartnoll and A. Tavanfar, “Electron stars for holographic metallic criticality,” arXiv:1008.2828 [hep-th].
- C. P. Herzog, **J. Phys. A** **42**, 343001 (2009) [arXiv:0904.1975 [hep-th]];
- C. P. Herzog, I. R. Klebanov, S. S. Pufu and T. Tesileanu, “Emergent Quantum Near-Criticality from Baryonic Black Branes,” arXiv:0911.0400 [hep-th].

- T. Holstein, R. E. Norton and P. Pincus, “de Haas-van Alphen Effect and the Specific Heat of an Electron Gas,” *Phys. Rev. B* **8**, 2649 (1973).
- G. T. Horowitz, arXiv:1002.1722 [hep-th].
- G. T. Horowitz and M. M. Roberts, “Zero Temperature Limit of Holographic Superconductors,” *JHEP* **0911** (2009) 015 [arXiv:0908.3677 [hep-th]].
- N. Iqbal and H. Liu, “Real-Time Response in AdS/CFT with Application to Spinors,” *Fortsch. Phys.* **57** (2009) 367 [arXiv:0903.2596 [hep-th]].
- N. Iqbal, H. Liu, M. Mezei and Q. Si, “Quantum phase transitions in holographic models of magnetism and superconductors,” *Phys. Rev. D* **82**, 045002 (2010) [arXiv:1003.0010 [hep-th]].
- S. Kachru, X. Liu and M. Mulligan, “Gravity Duals of Lifshitz-Like Fixed Points,” *Phys. Rev. D* **78** (2008) 106005 [arXiv:0808.1725 [hep-th]].
- Y. B. Kim, A. Furusaki, P. A. Lee, and X-G. Wen, “Gauge-invariant response functions of fermions coupled to a gauge field,” *Phys. Rev. B* **50**, 17917 (1994); Y. B. Kim, P. A. Lee, and X-G. Wen, “Quantum Boltzmann equation of composite fermions interacting with a gauge field” *Phys. Rev. B* **52**, 17275 (1995).
- M. Lawler et al, *Phys. Rev. B* **73**, 085101 (2006) [arXiv:cond-mat/0508747]; M. J. Lawler, E. Fradkin, *Phys. Rev. B* **75**, 033304 (2007) [arXiv:cond-mat/0605203].
- P. A. Lee and N. Nagaosa, “Gauge theory of the normal state of high-Tc superconductors,” *Phys. Rev. B* **46**, 5621 (1992).
- S. S. Lee, “A Non-Fermi Liquid from a Charged Black Hole: A Critical Fermi Ball,” arXiv:0809.3402 [hep-th].
- S. S. Lee, “Low energy effective theory of Fermi surface coupled with U(1) gauge field in 2+1 dimensions,” *Phys. Rev. B* **80**, 165102 (2009) [arXiv:0905.4532 [cond-mat.str-el]].
- H. Liu, J. McGreevy and D. Vegh, “Non-Fermi Liquids from Holography,” arXiv:0903.2477 [hep-th].
- G. Mahan, *Many-Particle Physics*, Plenum Press.
- J. M. Maldacena, “The large N limit of superconformal field theories and supergravity,” *Adv. Theor. Math. Phys.* **2**, 231 (1998);
- J. McGreevy, “Holographic Duality with a View Toward Many-Body Physics,” *Adv. High Energy Phys.* **2010**, 723105 (2010) [arXiv:0909.0518 [hep-th]].
- M. A. Metlitski and S. Sachdev, “Quantum phase transitions of metals in two spatial dimensions: I. Ising-nematic order,” *Phys. Rev. B* **82**, 075127 (2010) [arXiv:1001.1153 [cond-mat.str-el]].
- D. F. Mross, J. McGreevy, H. Liu and T. Senthil, “A controlled expansion for certain non-Fermi liquid metals,” *Phys. Rev. B* **82**, 045121 (2010) [arXiv:1003.0894 [cond-mat.str-el]].
- C. P. Nave and P. A. Lee, “Transport properties of a spinon Fermi surface coupled to a U(1) gauge field,” *Phys. Rev. B* **76**, 235124 (2007).
- C. Nayak and F. Wilczek, “Non-Fermi liquid fixed point in (2+1)-dimensions,” *Nucl. Phys. B* **417**, 359 (1994) arXiv:cond-mat/9312086, “Renormalization group approach to low temperature properties of a non-Fermi liquid metal,” *Nucl. Phys. B* **430**, 534 (1994) arXiv:cond-mat/9408016.
- V. Oganesyan, S. Kivelson, E. Fradkin, “Quantum Theory of a Nematic Fermi Fluid,” *Phys. Rev. B* **64**, 195109 (2001), arXiv:cond-mat/0102093v2 [cond-mat.str-el].
- J. Polchinski, “Effective Field Theory and the Fermi Surface,” arXiv:hep-th/9210046.
- J. Polchinski, “Low-energy dynamics of the spinon gauge system,” *Nucl. Phys. B* **422**, 617 (1994) arXiv:cond-mat/9303037.
- M. Y. Reizer, “Relativistic effects in the electron density of states, specific heat, and the electron

- spectrum of normal metals,” Phys. Rev. B **40**, 11571 (1989).
- S. J. Rey, “String Theory on Thin Semiconductors,” Progress of Theoretical Physics Supplement No. 177 (2009) pp. 128-142; arXiv:0911.5295 [hep-th].
- S. Sachdev and M. Mueller, “Quantum Criticality and Black Holes,” arXiv:0810.3005 [cond-mat.str-el].
- S. Sachdev, “Condensed matter and AdS/CFT,” arXiv:1002.2947 [hep-th].
- S. Sachdev, “Holographic metals and the fractionalized Fermi liquid,” arXiv:1006.3794 [hep-th].
- T. Schafer and K. Schwenzer, “Non-Fermi liquid effects in QCD at high density,” Phys. Rev. D **70**, 054007 (2004) arXiv:hep-ph/0405053.
- R. Shankar, Rev. Mod. Phys. **66**, 129 (1994).
- E. Silverstein, “TASI/PiTP/ISS lectures on moduli and microphysics,” arXiv:hep-th/0405068;
- D. T. Son and A. O. Starinets, “Minkowski-Space Correlators in AdS/CFT Correspondence: Recipe and Applications,” JHEP **0209** (2002) 042 [arXiv:hep-th/0205051].
- M. Spradlin and A. Strominger, “Vacuum states for AdS(2) black holes,” JHEP **9911**, 021 (1999) [arXiv:hep-th/9904143].
- C. M. Varma, P. B. Littlewood, S. Schmitt-Rink, E. Abrahams and A. E. Ruckenstein, “Phenomenology of the normal state of Cu-O high-temperature superconductors,” Phys. Rev. Lett. **63**, 1996 (1989).
- D. Vegh, “Fermi arcs from holography,” arXiv:1007.0246 [hep-th].
- E. Witten, “Anti-de Sitter space, thermal phase transition, and confinement in gauge theories,” Adv. Theor. Math. Phys. **2** *ibid.* 505 (1998);
- S. J. Yamamoto and Q. Si, “Global Phase Diagram of the Kondo Lattice: From Heavy Fermion Metals to Kondo Insulators,” J. Low Temp. Phys. **161**, 233 (2010); arXiv:1006.4868.